Journal of Human Genetics (2019) 64:521–534
https://doi.org/10.1038/s10038-019-0584-6

ARTICLE

# Gene regulation by antitumor *miR-130b-5p* in pancreatic ductal adenocarcinoma: the clinical significance of oncogenic *EPS8*

Haruhi Fukuhisa[1] · Naohiko Seki[2] · Tetsuya Idichi[1] · Hiroshi Kurahara[1] · Yasutaka Yamada[2] · Hiroko Toda[1] · Yoshiaki Kita[1] · Yota Kawasaki[1] · Kiyonori Tanoue[1] · Yuko Mataki[1] · Kosei Maemura[1] · Shoji Natsugoe[1]

Received: 3 January 2019 / Revised: 7 February 2019 / Accepted: 7 February 2019 / Published online: 11 March 2019


## Abstract

Our ongoing analyses identifying dysregulated microRNAs (miRNAs) and their controlled target RNAs have shed light on novel oncogenic pathways in pancreatic ductal adenocarcinoma (PDAC). The PDAC miRNA signature obtained by RNA sequencing showed that both strands of pre-*miR-130b* (*miR-130b-5p*, the passenger strand and *miR-130b-3p*, the guide strand) were significantly downregulated in cancer tissues. Our functional assays revealed that *miR-130b-5p* significantly blocked the malignant abilities of PDAC cell lines (PANC-1 and SW1990), e.g., cancer cell proliferation, migration, and invasion. A total of 103 genes were identified as possible oncogenic targets by *miR-130b-5p* regulation in PDAC cells based on genome-wide gene expression analysis and in silico database search. Among the possible targets, high expression of 9 genes (*EPS8*, *ZWINT*, *SMC4*, *LDHA*, *GJB2*, *ZCCHC24*, *TOP2A*, *ANLN*, and *ADCY3*) predicted a significantly poorer prognosis of PDAC patients (5-year overall survival, $p < 0.001$). Furthermore, we focused on *EPS8* because its expression had the greatest impact on patient prognosis (overall survival, $p < 0.0001$). Overexpression of *EPS8* was detected in PDAC clinical specimens. Knockdown assays with si*EPS8* showed that its overexpression enhanced cancer cell proliferation, migration, and invasion. Analysis of downstream RNA networks regulated by *EPS8* indicated that *MET*, *HMGA2*, *FERMT1*, *RARRES3*, *PTK2*, *MAD2L1*, and *FLI1* were closely involved in PDAC pathogenesis. Genes regulated by antitumor *miR-130b-5p* were closely involved in PDAC molecular pathogenesis. Our approach, discovery of antitumor miRNAs and their target RNAs, will contribute to exploring the causes of this malignant disease.

## Introduction

Due to a lack of early diagnostic strategies and its aggressive nature, pancreatic ductal adenocarcinoma (PDAC) is one of the most lethal cancers known to medicine [1]. Treatment options for locally advanced or metastatic PDAC are limited, and the median life expectancy is 6–11 months and 3–6 months for patients presenting with locally advanced disease or metastatic disease, respectively [2, 3]. Searching for new therapeutic targets and developing useful prognostic molecular markers are important goals to improve treatment outcomes of PDAC.

MicroRNAs (miRNAs) are small noncoding RNAs 19–24 nucleotides in length. They regulate gene expression by repressing translation or by cutting mRNAs in a sequence-dependent manner [4–6]. A single miRNA species is capable of modulating many protein-coding and noncoding RNA transcripts [7–9]. Thus, aberrantly expressed miRNAs can disrupt normal cell function, including supporting cancer pathogenesis [7–9].

Based on our original miRNA expression signatures by current genomic approaches, including that for PDAC, we have identified RNA networks that are controlled by antitumor miRNAs in several cancers [10–15]. In PDAC cells, our previous studies demonstrated that *miR-375*, *miR-216b-3p*, *miR-217*, *miR-148a*, and *miR-124-3p* were downregulated in PDAC tissues and these miRNAs had tumor suppressing

**Supplementary information** The online version of this article (https://doi.org/10.1038/s10038-019-0584-6) contains supplementary material, which is available to authorized users.

✉ Naohiko Seki
naoseki@faculty.chiba-u.jp

[1] Department of Digestive Surgery, Breast and Thyroid Surgery, Graduate School of Medical and Dental Sciences, Kagoshima University, Kagoshima, Japan

[2] Department of Functional Genomics, Chiba University Graduate School of Medicine, Chiba, Japan

functions, including controlling various oncogenes in PDAC cells [14, 16–19].

For example, expression of anillin (*ANLN*), actin-binding protein was directly controlled by *miR-217* and aberrant expression of *ANLN* promoted to cancer cell migration and invasion capabilities of PDAC cell lines [17]. Ectopic expression of *miR-124-3p* attenuated cancer cell aggressiveness through targeting oncogenic signaling via FAK, AKT, and ERK in PDAC cells [19]. Integrin α3 (*ITGA3*) and integrin β1 (*ITGB1*) were direct targets of *miR-124-3p* regulation in PDAC cells [19]. These findings suggest that analyses of antitumor miRNAs that regulate RNA networks will enhance understanding of PDAC molecular pathogenesis.

In this study, we focused on the passenger and guide strands of the *miR-130b* duplex *(miR-130b-5p*, the passenger strand and *miR-130b-3p*, the guide strand) based on miRNA expression signature of PDAC by RNA sequencing. Involvement of passenger strands of miRNAs is a new concept of miRNA biogenesis and these miRNAs provide the opportunity to find new regulatory networks in cancer cells. Here, we investigated the antitumor roles of *miR-130b-5p*, and their regulated oncogenic genes in PDAC pathogenesis.

## Materials and methods

### Human PDAC clinical specimens and cell lines

The present study was approved by the Bioethics Committee of Kagoshima University (Kagoshima, Japan; approval no. 160038 28-65). Written prior informed consent and approval were obtained from all of the patients.

In this study, 31 PDAC clinical samples were collected from PDAC patients who underwent resection at Kagoshima University Hospital from 1997 to 2016. Fifteen normal pancreatic tissue specimens were collected from non-cancerous regions. The clinical samples were staged according to the American Joint Committee on Cancer/Union Internationale Contre le Cancer (UICC) TNM classification. Clinical features in PDAC specimens are shown in Supplemental Table 1.

We used two PDAC cell lines: SW1990, purchased from the American Type Culture Collection (Manassas, VA, USA), and PANC-1, purchased from RIKEN Cell Bank (Tsukuba, Ibaraki, Japan).

### Quantitative real-time reverse transcription polymerase chain reaction (qRT-PCR)

The procedure for qRT-PCR has been described previously [17–21]. TaqMan qRT-PCR probes were obtained from Thermo Fisher Scientific (Waltham, MA, USA) as follows: *miR-130b-5p* (product ID: 002114), *miR-130b-3p* (product ID: 00456) and *EPS8* (product ID: Hs00610286_mH). *GUSB* (product ID: Hs99999908_m1) and *RNU48* (product ID: 001006) were used as internal controls.

### Transfection of mimic and inhibitor miRNA, small interfering RNA (siRNA) into PDAC cells

The following mature miRNAs and siRNAs were transfected into PDAC cells (PANC-1 and SW1990): *miR-130b-5p* (product ID: PM12970, Applied Biosystems, Foster City, CA, USA), *miR-130b-3p* (product ID: PM10777, Applied Biosystems) and Stealth Select RNAi siRNA, *EPS8* siRNAs (product IDs: HSS103325 and HSS103326, Invitrogen, Carlsbad, CA, USA). The transfection procedures were described in previous studies [20–25].

### Incorporation of *miR-130b-5p* into the RISC: assessment by Ago2 immunoprecipitation

Agonaute-2 (Ago2) is an essential components of the RNA-induced silencing complex (RISC) that binds to miRNAs. miRNAs were transfected into PANC-1 cells and were isolated using a microRNA Isolation Kit, Human Ago2 (Wako Pure Chemical Industries, Ltd., Osaka, Japan) as described previously [22–25]. The expression levels of Ago2-conjugated miRNAs were assessed by qRT-PCR assay.

### Cell proliferation, migration, and invasion assays

Functional assays for determining cell proliferation, migration, and invasion were described previously [16–19].

### Identification of putative oncogenic target genes regulated by *miR-130b-5p* in PDAC cells

To identify *miR-130b-5p*-controlled oncogenes, the following data sets were used: genome-wide gene expression analyses using PDAC cells transfected with *miR-130b-5p* predicted putative target genes that have *miR-130b-5p* binding sites in their 3' untranslated regions (TargetScan database ver. 7.1) and gene expression data of PDAC clinical specimens (Gene Expression Omnibus dataset: GEO accession number, GSE15471). Gene expression data (*miR-130b-5p* transfected PANC-1 cells) were deposited into the GEO database (accession number: GSE115801). An outline of the approach is shown in Supplemental Fig. 1 and was described in previous studies [20–25].

### Exploration of downstream targets regulated by si-*EPS8* in PDAC cells

Genome-wide gene expression and database oriented in silico analyses were applied to identify *EPS8*-mediated downstream genes. Outlines of the strategies were described in our previous studies [17, 18, 20, 21]. Our target search strategy in this study is shown in Supplemental Fig. 2. Gene expression data were deposited in GEO database (accession number: GSE118966).

### PDAC clinical data analysis by TCGA database

TCGA database was used to investigate the clinical significance of PDAC miRNAs and the genes they regulated (https://tcga-data.nci.nih.gov/tcga/). Gene expression and clinical data were obtained from cBioPortal (http://www.cbioportal.org/) and OncoLnc (http://www.oncolnc.org) (data downloaded on April 28, 2018). Detailed information on the databases were described in the previous papers [26–28].

### Western blot analysis and immunohistochemistry

The procedures for western blotting and immunohistochemistry were described in previous studies [17–19]. These assays used the following antibodies: anti-EPS8 (product ID: #43114, Cell Signaling Technology, Danvers, MA, USA) and anti-GAPDH (product ID: SAF6698, Wako).

Tissue sections were incubated overnight at 4 °C with anti-EPS8 antibodies diluted 1:400 (HPA003897; Sigma-Aldrich, St. Louis, MO, USA).

### Luciferase reporter assays

The following 2 sequences were cloned into the psiCHECk-2 vector (C8021; Promega Corporation, Madison, WI, USA): the wild-type sequence of the 3'-untranslated regions (UTRs) of *EPS8*, or the deletion-type, which lacked the *miR-130b-5p* target sites from *EPS8* (position 713–719). The procedures for transfection and dual luciferase reporter assays were provided in previous studies [20–25].

### Statistical analysis

To assess the significance of differences between 2 groups, we used Mann–Whitney *U*-tests. Differences between multiple groups were assessed by one-way ANOVA and Tukey tests for post-hoc analysis. We evaluated the correlations between the expression levels of *miR-130b-5p* and *EPS8* using Spearman's rank test. Tests utilized Expert StatView version 5.0 (SAS Institute, Inc., Cary, NC, USA) and JMPPro 14.0.0 (SAS Institute, Inc., Cary, NC, USA).

## Results

### Downregulation of *miR-130b-5p* and *miR-130b-3p* in PDAC clinical specimens and cell lines

We performed qRT-PCR to evaluate the expression levels of *miR-130b-5p* and *miR-130b-3p* in PDAC tissues ($n = 31$) as well as in normal pancreatic tissues ($n = 15$) and in 2 PDAC cell lines (PANC-1 and SW1990). Clinical features of the patients are summarized in Supplemental Table 1.

The expression levels of *miR-130b-5p* and *miR-130b-3p* were significantly downregulated in cancer tissues ($p = 0.0005$ and $p = 0.0009$; Fig. 1a). Spearman's rank test showed a positive correlation between the expression levels of *miR-130b-5p* and *miR-130b-3p* ($p < 0.0001$, $r = 0.875$; Fig. 1b).

In 2 cancer cell lines, PANC-1 and SW1990, the expression levels of *miR-130b-5p* and *miR-130b-3p* were extremely low (Fig. 1a).

### Effects of ectopic expression of *miR-130b-5p* and *miR-130b-3p* on PDAC cells

To verify the antitumor roles of *miR-130b-5p* and *miR-130b-3p*, we conducted gain-of-function studies by miRNA transfection into PANC-1 and SW1990 cells.

In cell proliferation assays, the inhibition of cancer cell growth was only detected with *miR-130b-5p* transfection into PANC-1 cells (Fig. 1c). Cell migration activities were reduced in the cells transfected with *miR-130b-5p* or *miR-130b-3p* (Fig. 1d).

Matrigel invasion assays revealed that transfection with *miR-130b-5p* or *miR-130b-3p* significantly decreased cell invasive capacity (Fig. 1e). However, no change was observed in *miR-130b-3p* transfection into PANC-1 cells (Fig. 1e).

### Incorporation of *miR-130b-5p* and *miR-130b-3p* into the RISC in PDAC cells

Ago2 is an essential component of the RISC. We hypothesized that the *miR-130b-3p* passenger strand in PDAC cells might be incorporated into the RISC where it could act as a tumor suppressor. To test that possibility, Ago2 was immunoprecipitated from PANC-1 cells that had been transfected with either *miR-130b-5p* or *miR-130b-3p*. Following isolation of Ago2-bound miRNAs, they were analyzed by qRT-PCR to determine whether *miR-130b-5p* or *miR-130b-3p* or both were associated. In transfectants, we observed higher levels of *miR-130-5p* expression than in mock transfectants or miR-controls or *miR-130b-3p* ($p < 0.005$) (Supplemental Fig. 3).

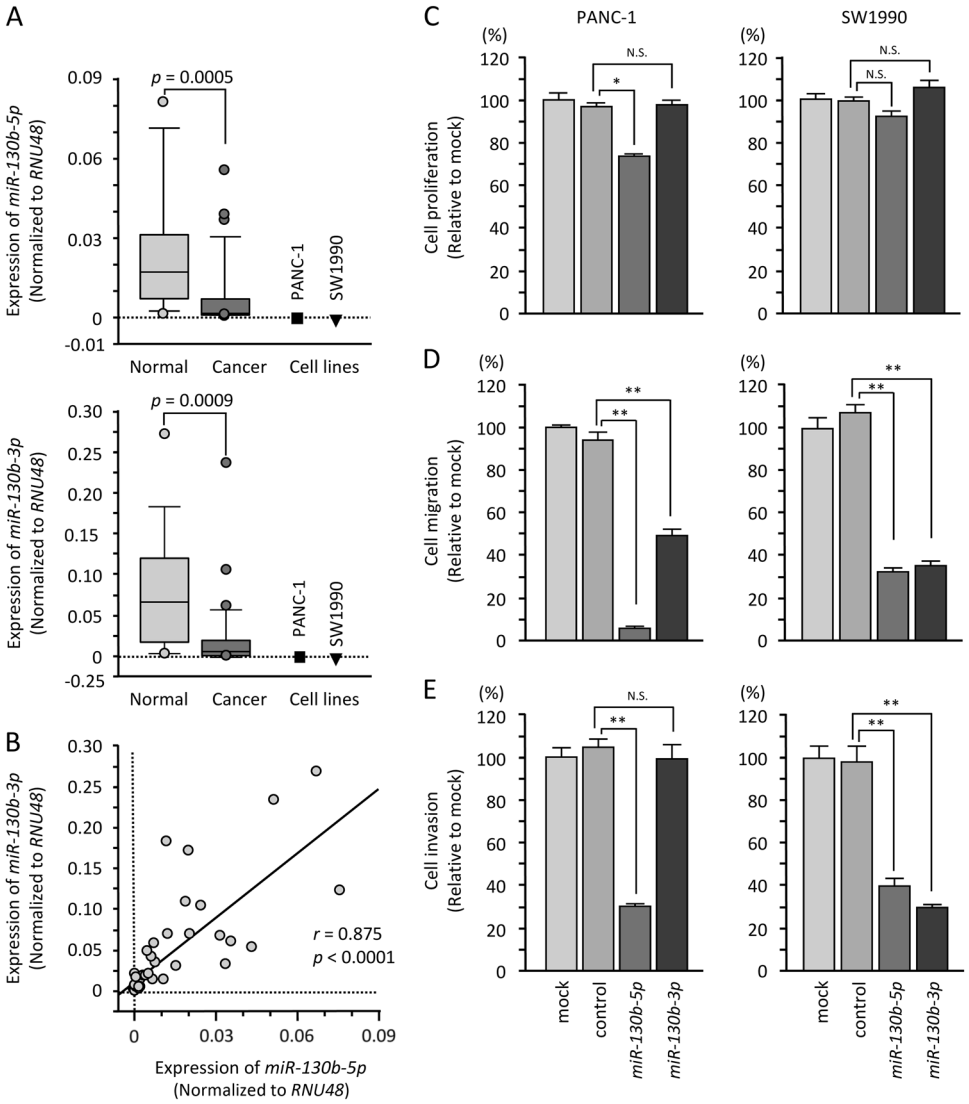


**Fig. 1** The functional significance of *miR-130b-5p* and *miR-130b-3p* in PDAC cells. **a** Expression levels of *miR-130b-5p* and *miR-130b-3p* in PDAC clinical specimens and cell lines (PANC-1 and SW1990). *RNU48* was used as an internal control. **b** Spearman's rank test demonstrated a positive correlation between the expression levels of *miR-130b-5p* and *miR-130b-3p*. **c**–**e** Effects of ectopic expression of *miR-130b-5p* and *miR-130b-3p* on PADC cells. **c** Cell proliferation was determined by XTT assays 72 h following transfection with *miR-130b-5p* or *miR-130b-3p*. **d** Results of cell migration assays. **e** Cell invasion activity was determined using Matrigel invasion assays. *, $p < 0.05$, **, $p < 0.0001$

## Identification of putative target genes controlled by *miR-130b-5p* in PDAC cells

To predict putative target genes controlled by *miR-130b-5p* in PDACs, we combined data from the following: genome-wide gene expression data (miR-*130b-5p* transfected into PANC-1 cells; GEO accession number: GSE115801), gene expression data from PDAC clinical specimens (GSE15471) and TargetScan database. The selection strategy of *miR-130b* targets is shown in Supplemental Fig. 1. A total of 103 genes were identified as putative *miR-130b-5p* controlled oncogenes in PDAC cells (Table 1).

To investigate the relationship between these target genes and the course of PDAC, we examined these genes with TCGA database. Among these targets, high expression of 9 genes (*EPS8*, *ZWINT*, *SMC4*, *LDHA*, *GJB2*, *ZCCHC24*, *TOP2A*, *ANLN,* and *ADCY3*) was associated with poor prognosis (5-year overall survival rates: $p < 0.01$) (Fig. 2).

Below, we focused on *EPS8* (epidermal growth factor receptor kinase substrate 8) because its expression was the most significantly predicted poor prognosis of the PDAC patients (Table 2, Fig. 2).

## Expression of *EPS8* in PDAC clinical specimens and its clinical significance

The levels of *EPS8* mRNA were significantly upregulated in PDAC tissues (Fig. 3a), with a negative correlation between the expression of *EPS8* and *miR-130b-5p* ($p = 0.0191$, $r = -0.349$; Spearman's rank tests, Fig. 3b).

Cox hazard regression analyses assessed the clinical significance of *EPS8* expression for OS in patients with

**Table. 1** Identification of putative targets regulated by miR-130b-5p in PDAC cells

| Entrez GeneID | Gene symbol | Gene name | PANC-1 miR-130b-5p transfectants (FC log2 < −1.0) | GEO expression data (FC log2 > 1.0) | TCGA_OncoLnc OS *p*-value (5 years) |
|---|---|---|---|---|---|
| 2059 | *EPS8* | epidermal growth factor receptor pathway substrate 8 | −1.0391617 | 1.262866923 | <0.0001 |
| 11130 | *ZWINT* | ZW10 interacting kinetochore protein | −1.4909135 | 1.160421740 | 0.0003 |
| 10051 | *SMC4* | structural maintenance of chromosomes 4 | −1.1281776 | 1.047700587 | 0.0015 |
| 3939 | *LDHA* | lactate dehydrogenase A | −1.0913677 | 1.246741586 | 0.0016 |
| 2706 | *GJB2* | gap junction protein, beta 2, 26 kDa | −1.0175266 | 3.693487627 | 0.0026 |
| 219654 | *ZCCHC24* | zinc finger, CCHC domain containing 24 | −1.2267109 | 1.436259135 | 0.0030 |
| 7153 | *TOP2A* | topoisomerase (DNA) II alpha 170 kDa | −1.7036874 | 1.530197372 | 0.0036 |
| 54443 | *ANLN* | anillin, actin-binding protein | −1.3910149 | 1.729212966 | 0.0037 |
| 109 | *ADCY3* | adenylate cyclase 3 | −1.0753918 | 1.001151172 | 0.0049 |
| 9055 | *PRC1* | protein regulator of cytokinesis 1 | −1.3384857 | 1.066709683 | 0.0123 |
| 6241 | *RRM2* | ribonucleotide reductase M2 | −1.3087503 | 1.166394096 | 0.0195 |
| 55013 | *CCDC109B* | coiled-coil domain containing 109B | −1.1029720 | 1.947959079 | 0.0226 |
| 55601 | *DDX60* | DEAD (Asp-Glu-Ala-Asp) box polypeptide 60 | −1.5366727 | 1.557264649 | 0.0241 |
| 3691 | *ITGB4* | integrin, beta 4 | −1.2837483 | 1.231679083 | 0.0292 |
| 91404 | *SESTD1* | SEC14 and spectrin domains 1 | −1.6589893 | 1.389203339 | 0.0324 |
| 444 | *ASPH* | aspartate beta-hydroxylase | −1.1716107 | 1.401796296 | 0.0331 |
| 2687 | *GGT5* | gamma-glutamyltransferase 5 | −1.1898923 | 1.128895036 | 0.0482 |
| 56925 | *LXN* | latexin | −1.4351722 | 2.047098603 | 0.0493 |
| 6772 | *STAT1* | signal transducer and activator of transcription 1, 91 kDa | −1.6604798 | 1.565144996 | 0.0521 |
| 26509 | *MYOF* | myoferlin | −1.1385632 | 2.424595363 | 0.0576 |
| 8777 | *MPDZ* | multiple PDZ domain protein | −1.2851086 | 1.089011295 | 0.0668 |
| 26031 | *OSBPL3* | oxysterol binding protein-like 3 | −1.7567873 | 1.636320355 | 0.0713 |
| 1601 | *DAB2* | Dab, mitogen-responsive phosphoprotein, homolog 2 (Drosophila) | −1.0613184 | 1.035552758 | 0.0780 |
| 55075 | *UACA* | uveal autoantigen with coiled-coil domains and ankyrin repeats | −2.4191770 | 1.278520676 | 0.0820 |
| 3339 | *HSPG2* | heparan sulfate proteoglycan 2 | −1.2415609 | 1.080375168 | 0.0920 |
| 80896 | *NPL* | N-acetylneuraminate pyruvate lyase (dihydrodipicolinate synthase) | −1.2635889 | 1.655438663 | 0.0950 |
| 79718 | *TBL1XR1* | transducin (beta)-like 1 × -linked receptor 1 | −1.2307795 | 1.018410917 | 0.0983 |
| 9749 | *PHACTR2* | phosphatase and actin regulator 2 | −1.9079069 | 1.021019626 | 0.1046 |
| 2745 | *GLRX* | glutaredoxin (thioltransferase) | −1.4243727 | 1.281624074 | 0.1083 |
| 5954 | *RCN1* | reticulocalbin 1, EF-hand calcium binding domain | −1.2084924 | 1.477113971 | 0.1103 |
| 79026 | *AHNAK* | AHNAK nucleoprotein | −1.3486654 | 1.085859303 | 0.1105 |
| 4628 | *MYH10* | myosin, heavy chain 10, non-muscle | −1.0401611 | 1.142164874 | 0.1230 |
| 2115 | *ETV1* | ets variant 1 | −1.0961652 | 2.305703430 | 0.1239 |
| 51316 | *PLAC8* | placenta-specific 8 | −1.7858686 | 1.696441959 | 0.1257 |
| 5357 | *PLS1* | plastin 1 | −1.0227555 | 1.122732612 | 0.1294 |
| 54933 | *RHBDL2* | rhomboid, veinlet-like 2 (Drosophila) | −1.4695596 | 1.179296700 | 0.1424 |
| 145389 | *SLC38A6* | solute carrier family 38, member 6 | −1.2434853 | 1.472348434 | 0.1577 |

**Table 1** (continued)

| Entrez GeneID | Gene symbol | Gene name | PANC-1 miR-130b-5p transfectants (FC log2 < −1.0) | GEO expression data (FC log2 > 1.0) | TCGA_OncoLnc OS *p*-value (5 years) |
|---|---|---|---|---|---|
| 54492 | *NEURL1B* | neuralized E3 ubiquitin protein ligase 1B | −1.2289410 | 1.235943540 | 0.1680 |
| 1687 | *DFNA5* | deafness, autosomal dominant 5 | −2.4118986 | 1.348055613 | 0.1707 |
| 5159 | *PDGFRB* | platelet-derived growth factor receptor, beta polypeptide | −1.6300844 | 1.799063012 | 0.1902 |
| 5738 | *PTGFRN* | prostaglandin F2 receptor inhibitor | −1.1871296 | 1.402088540 | 0.1939 |
| 4093 | *SMAD9* | SMAD family member 9 | −1.0708561 | 1.171259102 | 0.2192 |
| 57182 | *ANKRD50* | ankyrin repeat domain 50 | −1.5082961 | 1.240194756 | 0.2229 |
| 3696 | *ITGB8* | integrin, beta 8 | −1.1564417 | 1.573789775 | 0.2358 |
| 3434 | *IFIT1* | interferon-induced protein with tetratricopeptide repeats 1 | −1.5218506 | 1.277047673 | 0.2408 |
| 399474 | *TMEM200B* | transmembrane protein 200B | −2.0416780 | 1.009604441 | 0.2464 |
| 57674 | *RNF213* | ring finger protein 213 | −2.5736365 | 1.497929762 | 0.2474 |
| 64754 | *SMYD3* | SET and MYND domain containing 3 | −1.0121193 | 1.150962145 | 0.2509 |
| 57157 | *PHTF2* | putative homeodomain transcription factor 2 | −1.4924613 | 1.303249973 | 0.2571 |
| 84441 | *MAML2* | mastermind-like 2 (Drosophila) | −1.3098994 | 1.333379651 | 0.2598 |
| 1311 | *COMP* | cartilage oligomeric matrix protein | −1.1994047 | 3.571660308 | 0.2606 |
| 401494 | *PTPLAD2* (*HACD4*) | protein tyrosine phosphatase-like A domain containing 2 | −1.0844336 | 1.548839438 | 0.2682 |
| 5552 | *SRGN* | serglycin | −1.4376887 | 1.491958762 | 0.2782 |
| 130271 | *PLEKHH2* | pleckstrin homology domain containing, family H (with MyTH4 domain) member 2 | −2.2517653 | 1.262299887 | 0.2824 |
| 441168 | *FAM26F* | family with sequence similarity 26, member F | −1.0591393 | 1.170626686 | 0.2829 |
| 5176 | *SERPINF1* | serpin peptidase inhibitor, clade F (alpha-2 antiplasmin, pigment epithelium derived factor), member 1 | −1.0058947 | 1.339027896 | 0.3265 |
| 29969 | *MDFIC* | MyoD family inhibitor domain containing | −1.4263206 | 1.208129409 | 0.3845 |
| 3433 | *IFIT2* | interferon-induced protein with tetratricopeptide repeats 2 | −1.3565645 | 1.460924272 | 0.3916 |
| 7046 | *TGFBR1* | transforming growth factor, beta receptor 1 | −1.7564989 | 1.567228059 | 0.4061 |
| 9638 | *FEZ1* | fasciculation and elongation protein zeta 1 (zygin | −1.3657641 | 1.195616141 | 0.4099 |
| 10403 | *NDC80* | NDC80 kinetochore complex component | −1.2600021 | 1.547317152 | 0.4113 |
| 259232 | *NALCN* | sodium leak channel, non selective | −2.0426240 | 1.721556315 | 0.4212 |
| 7464 | *CORO2A* | coronin, actin-binding protein, 2A | −1.1782600 | 1.035525733 | 0.4377 |
| 10687 | *PNMA2* | paraneoplastic Ma antigen 2 | −1.2503138 | 2.060441736 | 0.4674 |
| 114882 | *OSBPL8* | oxysterol binding protein-like 8 | −1.2117767 | 1.080635358 | 0.4699 |
| 3912 | *LAMB1* | laminin, beta 1 | −1.1625280 | 1.678489460 | 0.4837 |
| 29887 | *SNX10* | sorting nexin 10 | −1.1817684 | 1.203410167 | 0.4885 |
| 4053 | *LTBP2* | latent transforming growth factor beta binding protein 2 | −1.1001697 | 1.700059684 | 0.4888 |
| 57333 | *RCN3* | reticulocalbin 3, EF-hand calcium binding domain | −1.0096655 | 1.209374756 | 0.5065 |

**Table 1** (continued)

| Entrez GeneID | Gene symbol | Gene name | PANC-1 miR-130b-5p transfectants (FC log2 < −1.0) | GEO expression data (FC log2 > 1.0) | TCGA_OncoLnc OS *p*-value (5 years) |
|---|---|---|---|---|---|
| 57480 | *PLEKHG1* | pleckstrin homology domain containing, family G (with RhoGef domain) member 1 | −1.3316975 | 1.567208536 | 0.5090 |
| 493869 | *GPX8* | glutathione peroxidase 8 (putative) | −2.4862900 | 2.136870238 | 0.5220 |
| 1122 | *CHML* | choroideremia-like (Rab escort protein 2) | −1.4233093 | 1.228576636 | 0.5285 |
| 8829 | *NRP1* | neuropilin 1 | −1.4793081 | 1.302180230 | 0.5412 |
| 8819 | *SAP30* | Sin3A-associated protein, 30 kDa | −1.0623255 | 1.094283911 | 0.5456 |
| 83879 | *CDCA7* | cell division cycle associated 7 | −1.2634476 | 1.318760386 | 0.5659 |
| 4921 | *DDR2* | discoidin domain receptor tyrosine kinase 2 | −1.0453687 | 1.487748419 | 0.5667 |
| 80328 | *ULBP2* | UL16 binding protein 2 | −2.3729725 | 1.235425992 | 0.5685 |
| 10123 | *ARL4C* | ADP-ribosylation factor-like 4C | −1.2759942 | 2.283123981 | 0.5705 |
| 55711 | *FAR2* | fatty acyl CoA reductase 2 | −1.2279121 | 1.048943407 | 0.5748 |
| 25878 | *MXRA5* | matrix-remodeling associated 5 | −1.1647496 | 2.386952616 | 0.5751 |
| 162073 | *ITPRIPL2* | inositol 1,4,5-trisphosphate receptor interacting protein-like 2 | −1.3766663 | 1.058793251 | 0.6025 |
| 8321 | *FZD1* | frizzled class receptor 1 | −1.7407991 | 1.186160064 | 0.6113 |
| 6443 | *SGCB* | sarcoglycan, beta (43 kDa dystrophin-associated glycoprotein) | −1.4844265 | 1.119623109 | 0.6616 |
| 23092 | *ARHGAP26* | Rho GTPase activating protein 26 | −1.8215991 | 1.471498081 | 0.6710 |
| 4815 | *NINJ2* | ninjurin 2 | −1.2982117 | 1.146017467 | 0.6778 |
| 30011 | *SH3KBP1* | SH3-domain kinase binding protein 1 | −1.3079715 | 1.652279466 | 0.6995 |
| 4175 | *MCM6* | minichromosome maintenance complex component 6 | −1.0063353 | 1.015316222 | 0.7117 |
| 5911 | *RAP2A* | RAP2A, member of RA oncogene family | −1.1328840 | 1.057927314 | 0.7322 |
| 9902 | *MRC2* | mannose receptor, C type 2 | −1.0907621 | 1.385321140 | 0.7776 |
| 133418 | *EMB* | embigin | −1.1111135 | 1.447293274 | 0.7843 |
| 84168 | *ANTXR1* | anthrax toxin receptor 1 | −1.1164263 | 2.902470068 | 0.8002 |
| 1287 | *COL4A5* | collagen, type IV, alpha 5 | −1.1768475 | 1.170016241 | 0.8029 |
| 8082 | *SSPN* | sarcospan | −1.5962458 | 1.133155515 | 0.8072 |
| 8543 | *LMO4* | LIM domain only 4 | −1.3773192 | 1.067641814 | 0.8208 |
| 10551 | *AGR2* | anterior gradient 2 | −1.2424725 | 2.048504817 | 0.8335 |
| 23271 | *CAMSAP2* | calmodulin regulated spectrin-associated protein family, member 2 | −1.0790195 | 1.378435602 | 0.8550 |
| 8324 | *FZD7* | frizzled class receptor 7 | −1.4669601 | 1.585164272 | 0.8594 |
| 4286 | *MITF* | microphthalmia-associated transcription factor | −1.6427531 | 1.117288105 | 0.8612 |
| 1475 | *CSTA* | cystatin A (stefin A) | −1.5165935 | 2.094066552 | 0.8674 |
| 90459 | *ERI1* | exoribonuclease 1 | −1.2428759 | 1.087664329 | 0.8894 |
| 1296 | *COL8A2* | collagen, type VIII, alpha 2 | −1.4797236 | 1.993645272 | 0.9346 |
| 80005 | *DOCK5* | dedicator of cytokinesis 5 | −1.0028888 | 1.203107167 | 0.9558 |
| 150759 | *LINC00342* | long intergenic non-protein coding RNA 342 | −1.1021174 | 1.414509394 | – |

PDAC. With multivariate analysis, we found that *EPS8* expression was an independent predictive factor for OS (hazard ratio = 1.893, $p = 0.0053$; Fig. 3c).

PDAC clinical specimens were subjected to immunohistochemical analyses. The results indicated that EPS8 protein was strongly expressed in cancer lesions. In

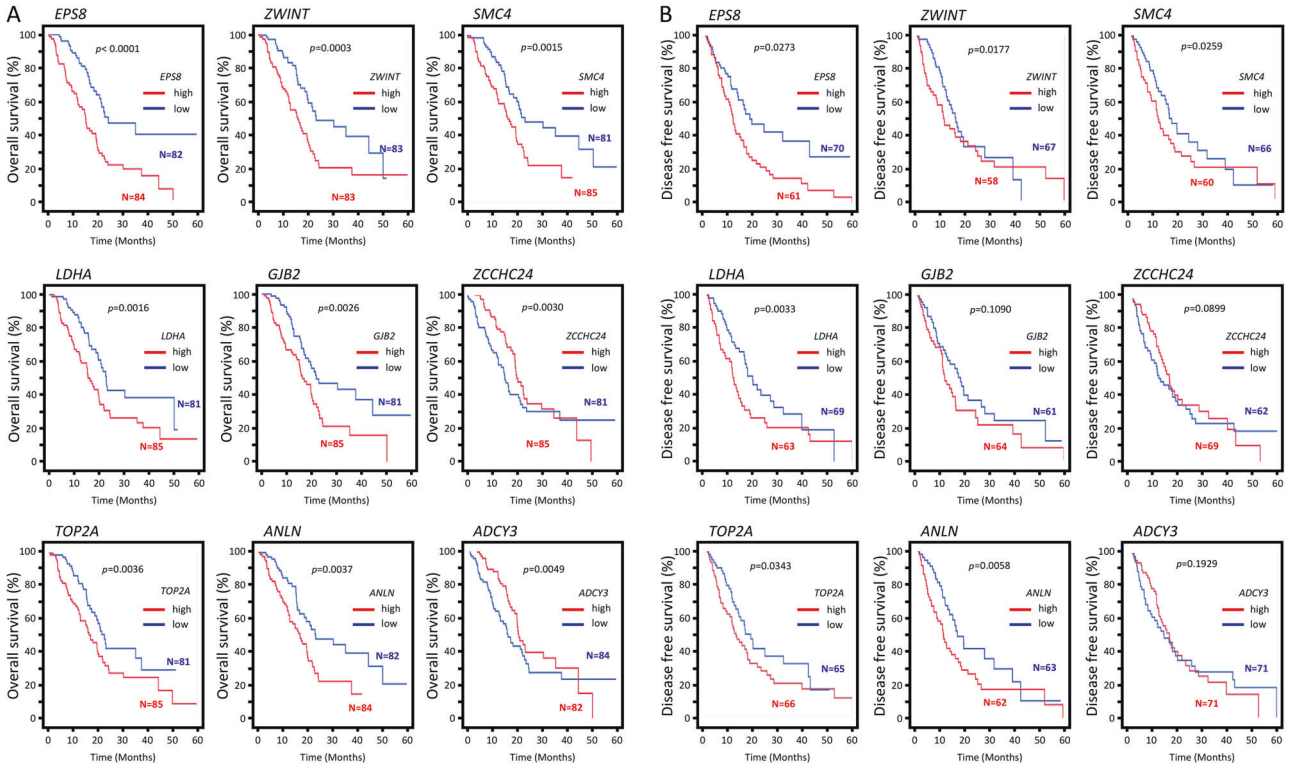


**Fig. 2** Clinical significance of the expression of 9 genes (*EPS8*, *ZWINT*, *SMC4*, *LDHA*, *GJB2*, *ZCCHC24*, *TOP2A*, *ANLN*, and *ADCY3*) based on The Cancer Genome Atlas (TCGA) database. Survival rate differences were analyzed by Kaplan–Meier survival curves and log-rank statistics. **a** Kaplan–Meier plots of overall survival and **b** disease-free survival with log-rank tests for genes with high and low expression from The Cancer Genome Atlas database

contrast, expression was infrequent and weak in normal pancreatic cells (Fig. 3d).

## Direct regulation of *EPS8* by *miR-130b-5p* in PDAC cells

In cells transfected with *miR-130b-5p*, the levels of *EPS8* mRNA and EPS8 protein were significantly lower than mock- or miR-control-transfected cells (Fig. 4a, b). Binding sites for *miR-130b-5p* in the 3'-UTR of *EPS8* (positions 713–719, Fig. 4c, upper) were predicted by the TargetScan database. We used luciferase reporter assays with vectors carrying either the wild-type or deletion-type 3'-UTR of *EPS8*. We observed greatly reduced luminescence after transfection with *miR-130b-5p* and the vector carrying the wild-type 3'-UTR of *EPS8*. Transfection with the deletion-type vector did not reduce luminescence intensities in PANC-1 and SW1990 cells. Thus, *miR-130b-5p* directly bound to *EPS8* in the 3'-UTR (Fig. 4c).

In addition, we investigated the effect of suppression of *EPS8*/EPS8 by *miR-130a-5p* (seed sequence is almost identical) in PDAC cells. Expression of *EPS8*/EPS8 was slightly suppressed by *miR-130a-5p* in PANC-1 and SW1990 (data not shown).

## Effects of silencing *EPS8* on PDAC cells

Next, we transfected siRNAs into PANC-1 and SW1990 cells to examine the function of *EPS8* in PDAC cells. The mRNA and protein expression levels of *EPS8*/EPS8 were decreased by si-*EPS8* (Supplemental Figs. 4A and 4B).

We examined the effects of knockdown of *EPS8* in PDAC cells, and found that cell proliferation was not affected (Fig. 4d). Cancer cell migration and invasive activities were significantly inhibited by si-*EPS8* transfection into PDAC cells, PANC-1 and SW1990. However, silencing of *EPS8* did not affect cell proliferation (Fig. 4d–f).

## Downstream genes affected by silencing of *EPS8* in PDAC cells

To identity downstream genes controlled by *EPS8*, we used two sets of genome-wide gene expression data (si-*EPS8* transfected cells: GSE118966 and PDAC expression data: GSE15471). Our selection strategy is shown in Supplemental Fig. 2.

In total, 48 genes were identified as putative downstream genes controlled by *EPS8* in PDAC cells (Table 2). Among 8 genes, high expression affected overall survival

**Table. 2** Identification of EP8 mediated downstream genes in PDAC cells

| Entrez GeneID | Gene symbol | Gene name | PANC-1 si-*EPS8* transfectants (FC log2 < −1.0) | GEO expression data (FC log2 > 1.0) | TCGA_OncoLnc OS *p*-value (5 years) |
|---|---|---|---|---|---|
| 2059 | *EPS8* | epidermal growth factor receptor pathway substrate 8 | −2.8271956 | 2.3997214 | <0.0001 |
| 4233 | *MET* | MET proto-oncogene, receptor tyrosine kinase | −1.0782841 | 2.8329950 | 0.0015 |
| 8091 | *HMGA2* | high mobility group AT-hook 2 | −2.3884200 | 2.4964874 | 0.0031 |
| 55612 | *FERMT1* | fermitin family member 1 | −1.3296491 | 3.1556027 | 0.0103 |
| 5920 | *RARRES3* | retinoic acid receptor responder (tazarotene induced) 3 | −1.1847581 | 2.8853405 | 0.0125 |
| 5747 | *PTK2* | protein tyrosine kinase 2 | −1.0931424 | 2.1476655 | 0.0134 |
| 4085 | *MAD2L1* | MAD2 mitotic arrest deficient-like 1 (yeast) | −1.3218220 | 2.2757983 | 0.0412 |
| 2313 | *FLI1* | Fli-1 proto-oncogene, ET transcription factor | −1.2141428 | 2.1929195 | 0.0443 |
| 3437 | *IFIT3* | interferon-induced protein with tetratricopeptide repeats 3 | −2.7479300 | 2.5652308 | 0.0574 |
| 84034 | *EMILIN2* | elastin microfibril interfacer 2 | −2.3441610 | 2.3126762 | 0.0868 |
| 3397 | *ID1* | inhibitor of DNA binding 1, dominant negative helix-loop-helix | −1.2009468 | 2.4448597 | 0.0969 |
| 79026 | *AHNAK* | AHNAK nucleoprotein | −1.3035727 | 2.1226394 | 0.1105 |
| 54739 | *XAF1* | XIAP associated factor 1 | −1.2250342 | 3.6524053 | 0.1327 |
| 7764 | *ZNF217* | zinc finger protein 217 | −1.0156298 | 2.1386855 | 0.1358 |
| 6286 | *S100 P* | S100 calcium binding protein P | −1.7940164 | 12.7159950 | 0.1515 |
| 6001 | *RGS10* | regulator of G-protein signaling 10 | −1.3992062 | 3.0485551 | 0.1700 |
| 5159 | *PDGFRB* | platelet-derived growth factor receptor, beta polypeptide | −2.2982244 | 3.4799414 | 0.1902 |
| 7220 | *TRPC1* | transient receptor potential cation channel, subfamily C, member 1 | −1.0543852 | 2.8364346 | 0.1999 |
| 23603 | *CORO1C* | coronin, actin-binding protein, 1C | −1.8096170 | 2.9602175 | 0.2026 |
| 330 | *BIRC3* | baculoviral IAP repeat containing 3 | −1.5710629 | 2.6069708 | 0.2322 |
| 3434 | *IFIT1* | interferon-induced protein with tetratricopeptide repeats 1 | −1.2829789 | 2.4234254 | 0.2408 |
| 57674 | *RNF213* | ring finger protein 213 | −2.2830563 | 2.8243713 | 0.2474 |
| 3915 | *LAMC1* | laminin, gamma 1 (formerly LAMB2) | −1.0173159 | 2.5432700 | 0.2490 |
| 659 | *BMPR2* | bone morphogenetic protein receptor, type II (serine/threonine kinase) | −2.0797455 | 2.4564056 | 0.3162 |
| 716 | *C1S* | complement component 1, s subcomponent | −1.3375945 | 4.1859550 | 0.3696 |
| 7498 | *XDH* | xanthine dehydrogenase | −1.0785036 | 2.2759452 | 0.3800 |
| 29969 | *MDFIC* | MyoD family inhibitor domain containing | −1.1913158 | 2.3103788 | 0.3845 |
| 3433 | *IFIT2* | interferon-induced protein with tetratricopeptide repeats 2 | −2.7081504 | 2.7528467 | 0.3916 |
| 7046 | *TGFBR1* | transforming growth factor, beta receptor 1 | −1.0406232 | 2.7592096 | 0.4061 |
| 259232 | *NALCN* | sodium leak channel, non selective | −1.8967161 | 3.2979198 | 0.4212 |
| 64859 | *NABP1* | nucleic acid binding protein 1 | −1.0262889 | 2.4854288 | 0.4593 |
| 29887 | *SNX10* | sorting nexin 10 | −1.0249023 | 2.3028336 | 0.4885 |
| 219285 | *SAMD9L* | sterile alpha motif domain containing 9-like | −1.2528054 | 2.2927480 | 0.5013 |

**Table 2** (continued)

| Entrez GeneID | Gene symbol | Gene name | PANC-1 si-*EPS8* transfectants (FC log2 < −1.0) | GEO expression data (FC log2 > 1.0) | TCGA_OncoLnc OS *p*-value (5 years) |
|---|---|---|---|---|---|
| 6453 | *ITSN1* | intersectin 1 (H3 domain protein) | −1.0911493 | 2.3252943 | 0.5098 |
| 253782 | *CERS6* | ceramide synthase 6 | −1.2245360 | 2.0965688 | 0.5536 |
| 727936 | *GXYLT2* | glucoside xylosyltransferase 2 | −2.9657586 | 4.1614670 | 0.5649 |
| 9120 | *SLC16A6* | solute carrier family 16, member 6 | −1.0826521 | 2.3125410 | 0.5799 |
| 1953 | *MEGF6* | multiple EGF-like-domains 6 | −1.4605589 | 2.2775905 | 0.5966 |
| 26064 | *RAI14* | retinoic acid induced 14 | −1.4694735 | 2.7101336 | 0.6374 |
| 6016 | *RIT1* | Ras-like without CAAX 1 | −1.1128588 | 2.2873511 | 0.6606 |
| 4026 | *LPP* | LIM domain containing preferred translocation partner in lipoma | −1.3406305 | 2.0011916 | 0.7361 |
| 1728 | *NQO1* | NAD(P)H dehydrogenase, quinone 1 | −1.2154182 | 4.5524726 | 0.8302 |
| 59339 | *PLEKHA2* | pleckstrin homology domain containing, family A (phosphoinositide binding specific) member 2 | −1.5718870 | 2.0061517 | 0.8335 |
| 1871 | *E2F3* | E2F transcription factor 3 | −1.0145493 | 2.4384596 | 0.8898 |
| 397 | *ARHGDIB* | Rho GDP dissociation inhibitor (GDI) beta | −1.5170516 | 3.2517672 | 0.9057 |
| 10365 | *KLF2* | Kruppel-like factor 2 | −1.7209059 | 2.0431898 | 0.9088 |
| 51056 | *LAP3* | leucine aminopeptidase 3 | −1.7265989 | 2.0905375 | 0.9187 |
| 1296 | *COL8A2* | collagen, type VIII, alpha 2 | −1.0540862 | 3.9824197 | 0.9346 |

rates ($p < 0.05$). Specifically, *MET*, *HMGA2*, *CORO1C*, *FERMT1*, *RARRES3*, *PTK2*, *MAD2L1,* and *FLI1* were significantly associated with poor prognosis in patients with PDAC by TCGA analysis (Table 2 and Supplemental Figure 5).

## Discussion

miRNAs have unique characteristics. For example, a single miRNA species can regulate vast numbers of RNA transcripts in normal and pathological cells. Expression of RNAs controlled by miRNA varies depending on the cell [7–9]. Therefore, identification of aberrantly expressed miRNAs and their targets is the first step in elucidating molecular pathogenesis in PDAC cells. Using our original miRNA signature of PDAC by RNA sequencing, the molecular network controlled by antitumor miRNAs in PCAD cells is being clarified [14, 16–19]. In this study, we focused on both strands of pre-*miR-130b* (*miR-130b-5p* and *miR-130b-3p*) because these miRNAs were significantly downregulated in our and other PDAC signatures [14, 29, 30].

Several miRNAs form families based on their seed sequences. The *miR-130* family consists of 4 miRNAs: *miR-130a* (chromosome 11q12.1), *miR-130b* (22q11.21), *miR-301a* (17q22), and *miR-301b* (22q11.21) [31–33]. The seed sequences of passenger strands *miR-130a-5p* and *miR-130b-5p* are almost identical. The seed sequences of guide strands of all member of the *miR-130* family (*miR-130a-3p*, *miR-130b-3p*, *miR-301a-3p* and *miR-301b-3p*) are identical (seed sequences are summarized in Supplemental Figure 6). Previous studies showed that a number of *miR-130* family (guide strands) were overexpressed in cancer tissues and their functions were involved in oncogenesis, e.g., bladder cancer, esophageal squamous cell carcinoma and lung cancer [32, 34, 35].

Contrary to these reports, *miR-130a* and *miR-130b* were downregulated in cancer tissues and they acted as antitumor miRNAs in ovarian cancer, prostate cancer, endometrial cancer, and papillary thyroid carcinoma [31, 33, 36, 37]. Our present data show that both strands (*miR-130b-5p* and *miR-130b-3p)* were significantly reduced in PDAC clinical specimens and cell lines. Furthermore, ectopic expression of these miRNAs inhibited malignant phenotypes in PDAC cells, suggesting that both *miR-130b-5p* and *miR-130b-3p* play antitumor roles in PDAC cells. In a previous study of PDAC cells, expression of *miR-130b-3p* was suppressed in cancer tissues and its expression was an independent prognostic predictor of the patients' disease course [38]. Overexpression of *miR-130b-3p* induced apoptotic cells through targeting of *STAT3* in PDAC cells [38]. These findings showed that *miR-130b* has multiple functions, oncogenic or antitumor roles depending on the specific cancer cell. It is indispensable to elucidate the molecular mechanism controlling *miR-130b* expression in several types of cancer cells.

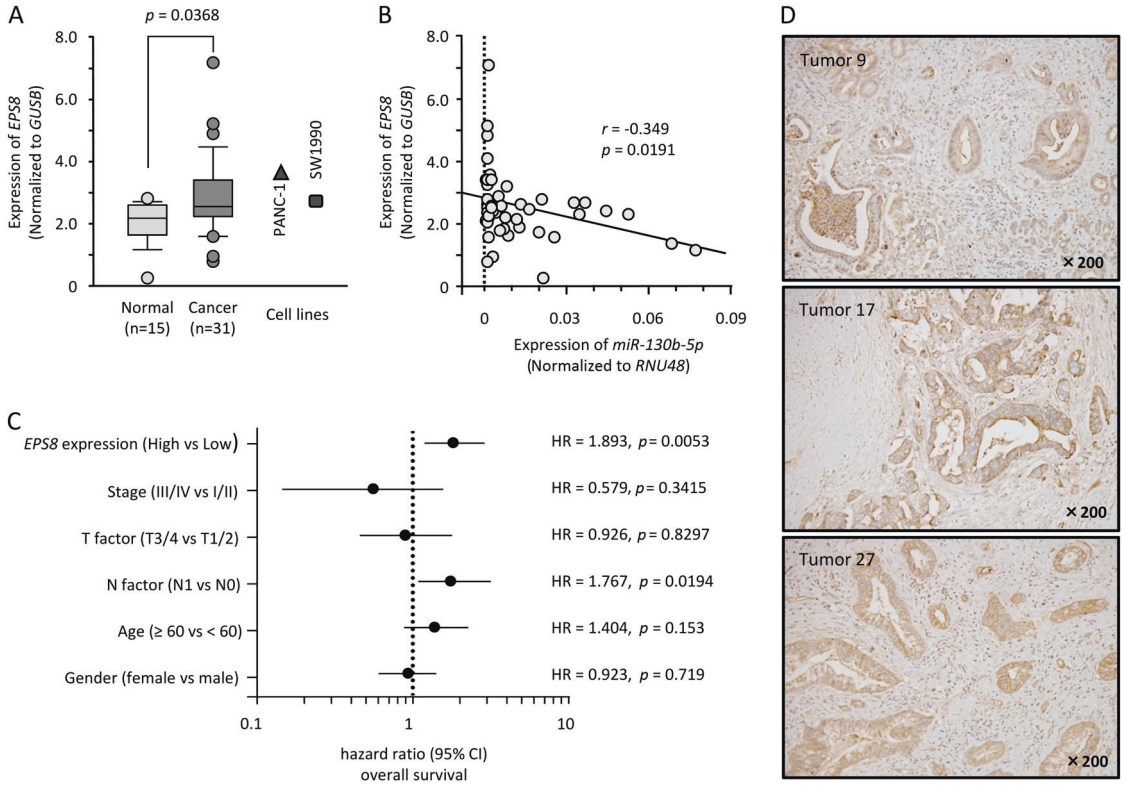


**Fig. 3** Aberrant expression of *EPS8* in PDAC specimens and its clinical significance. **a** Expression levels of *EPS8* in PDAC clinical specimens. *GUSB* was the internal control. **b** Spearman's rank test was used to evaluate the correlation between *EPS8* expression and *miR-130b-5p* expression in PDAC clinical specimens. **c** Analysis of the expression levels of *EPS8* in patients with PDAC using TCGA database. Forest plot of univariate Cox proportional hazards regression analysis of 5-year overall survival. Univariate and multivariate analyses for OS using TCGA database were carried out by Cox proportional hazards regression analyses. **d** Immunohistochemical analysis of PDAC clinical samples. EPS8 was strongly expressed in cancer lesions

Previous study showed that hyper-methylation of the promoter region of *miR-130b* was observed in ovarian cancer clinical tissues and cell lines and methylation cased to downregulation of *miR-130b* expression [31]. In prostate cancer, downregulation of *miR-130b/miR-301b* cluster was detected in clinical specimens and cell lines [33]. Methylation levels of their promoter region were significantly higher in prostate cancer tissues compared to normal tissues [33]. Expression levels of *miR-130b* and *miR-301b* were upregulated by treatment of demethylation drugs [33]. These findings showed that downregulation of *miR-130b* was mediated by aberrant methylation on its promoter region. For *miR-130* family, comprehensive analysis of the molecular mechanism of suppressing their expression in PDAC cells is indispensable.

This is the first report that *miR-130b-5p* (the passenger strand) acted as an antitumor miRNA in PDAC. Therefore, we focused on *miR-130b-5p* to investigate its control of oncogenes involved in PDAC pathogenesis. In this study, a total of 103 putative oncogenes were identified that were regulated by *miR-130b-5p* in PDAC cells. Among these targets, overexpression of 9 genes (*EPS8*, *ZWINT*, *SMC4*, *LDHA*, *GJB2*, *ZCCHC24*, *TOP2A*, *ANLN*, and *ADCY3*) were closely associated with poor prognosis of the patients with PDAC. Interestingly, aberrant expression of *ANLN* (actin-binding protein anillin) was detected in PDAC clinical specimens [17]. Knockdown assays of *ANLN* expression markedly inhibited cancer cell migration and invasive capabilities of PDAC cell lines [17]. In addition, *ANLN* was directly controlled by antitumor *miR-217* in PDAC cells [17].

Furthermore, we investigated the functional significance of *EPS8* (epidermal growth factor receptor pathway substrate 8) in PDAC cells. EPS8 binds several adaptor proteins and acts as a substrate for receptor and non-receptor tyrosine kinases, e.g., EGFR, FGFR, VEGFR, and Src [39]. Other studies showed that EPS8 has the actin-binding ability and it acts by capping barbed ends and promoting bundling [40]. Furthermore, EPS8 forms a trimer (EPS8, Abi-1 and SOS-1) and this complex acts as a guanine nucleotide exchange factor (GEFs) in Rac signaling and contributes to Rac-based actin polymerizing processes [41]. Aberrantly expressed *EPS8* was reported in colon cancer, breast cancer, hematologic malignancies, and cervical cancer, and its overexpression was closely involved in the malignant phenotype [42–45]. Our present data revealed

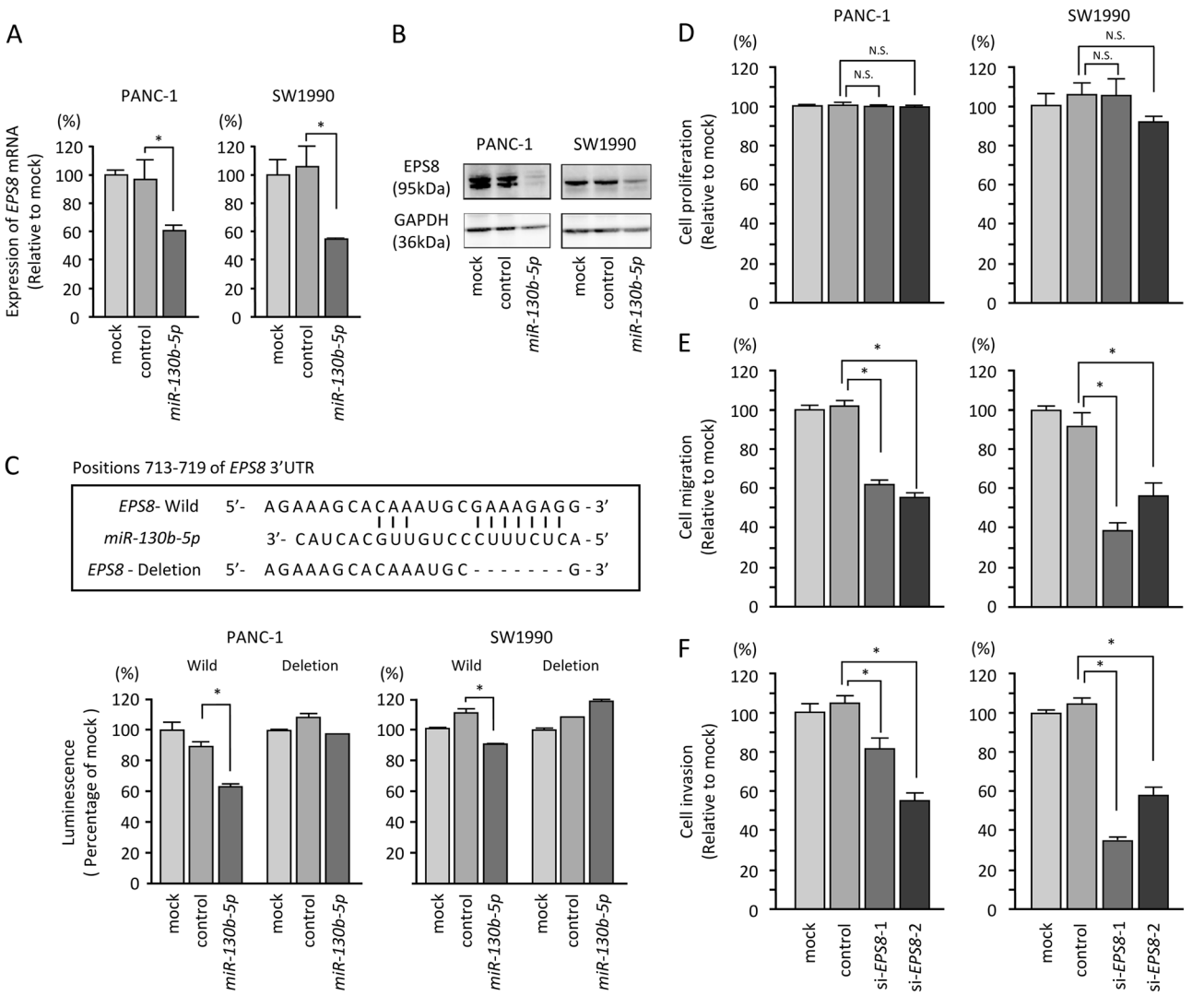


**Fig. 4** Oncogenic function of *EPS8* in PDAC cells. **a**, **b** *miR-130b-5p* directly regulated *EPS8* in PDAC cells. Expression levels of *EPS8* mRNA (**a**) or EPS8 protein (**b**) 72 h or 96 h following transfection with 10 nM *miR-130b-5p* into cell lines. **c** *miR-130b-5p* binding site (positions 713–719) in the 3'-UTR of *EPS8* mRNA. Dual luciferase reporter assays using vectors encoding putative *miR-130b-5p* target sites in the *EPS8* 3'-UTRs for both wild-type and deleted regions. *Renilla* luciferase values were normalized to firefly luciferase values. $*p < 0.005$. **d**–**f** Effects of silencing *EPS8* in PDAC cells. **d** Cell proliferation, **e** migration and **f** invasion assays. These assays showed that inhibition of migration and invasion were observed in si-*EPS8*-transfected cell lines (PANC-1 and SW1990). $*p < 0.005$

that *EPS8* regulated cancer cell migration and invasion and its expression is promising as a diagnostic marker for PDAC. Aberrant expression of *EPS8* might be a promising therapeutic target for PDAC.

Finally, to investigate the *EPS8*-mediated oncogenic genes and pathways in PDAC cells, we applied genome-wide gene expression analyses using knockdown of *EPS8* in cells. A total of 48 genes were identified as putative *EPS8*-mediated targets in PDAC cells. Surprisingly, aberrant expression of 7 genes (*MET*, *HMGA2*, *FERMT1*, *RARRES3*, *PTK2*, *MAD2L1*, and *FLI1*, $p < 0.05$) was closely associated with poor prognosis of patients with PADC. In this study, it was revealed that many of the genes controlled by antitumor *miR-130b-5p* and *ESP8*-mediated downstream genes were closely involved in the molecular pathogenesis of PDAC. Elucidation of novel RNA networks controlled by antitumor miRNAs will accelerate comprehensive understanding of molecular pathogenesis of PDAC.

In conclusion, our results showed that expression of both strands of the pre-*miR-130b* duplex were significantly downregulated in PDAC clinical specimens and thus the *miR-130b*-duplex could act as an antitumor miRNA in such cells. A total of 9 genes (*EPS8*, *ZWINT*, *SMC4*, *LDHA*, *GJB2*, *ZCCHC24*, *TOP2A*, *ANLN*, and *ADCY3*) were closely associated with PDAC pathogenesis. Among these targets, the aberrant expression of *EPS8* enhanced cancer aggressiveness, suggesting that *EPS8* could be a promising therapeutic target for PDAC. Our approach, discovery of

antitumor miRNAs and their target RNAs, will contribute to exploring the causes of this malignant disease.

**Acknowledgements** This study was supported by Japan Society for the Promotion of Science 17H04285, 18K08626, 18K08687, 18K16322, 18K09338, 16K19945, and 18K15219.

## Compliance with ethical standards

**Conflict of interest** The authors declare that they have no conflict of interest.



## References

1. Kamisawa T, Wood LD, Itoi T, Takaori K. Pancreatic cancer. Lancet. 2016;388:73–85.
2. Das S, Batra SK. Pancreatic cancer metastasis: are we being pre-EMTed? Curr Pharm Des. 2015;21:1249–55.
3. Polireddy K, Chen Q. Cancer of the pancreas: molecular pathways and current advancement in treatment. J Cancer. 2016; 7:1497–514.
4. Bartel DP. MicroRNAs: genomics, biogenesis, mechanism, and function. Cell . 2004;116:281–97.
5. Bartel DP. MicroRNAs: target recognition and regulatory functions. Cell . 2009;136:215–33.
6. Liu WW, Meng J, Cui J, Luan YS. Characterization and function of microRNA(*)s in plants. Front Plant Sci. 2017;8:2200.
7. Goto Y, Kurozumi A, Enokida H, Ichikawa T, Seki N. Functional significance of aberrantly expressed microRNAs in prostate cancer. Int J Urol. 2015;22:242–52.
8. Koshizuka K, Hanazawa T, Arai T, Okato A, Kikkawa N, Seki N. Involvement of aberrantly expressed microRNAs in the pathogenesis of head and neck squamous cell carcinoma. Cancer Metastas- Rev. 2017;36:525–45.
9. Yonemori K, Kurahara H, Maemura K, Natsugoe S. MicroRNA in pancreatic cancer. J Hum Genet. 2017;62:33–40.
10. Itesako T, Seki N, Yoshino H, Chiyomaru T, Yamasaki T, Hidaka H, et al. The microRNA expression signature of bladder cancer by deep sequencing: the functional significance of the miR-195/497 cluster. PLoS ONE. 2014;9:e84311.
11. Goto Y, Kurozumi A, Arai T, Nohata N, Kojima S, Okato A, et al. Impact of novel miR-145-3p regulatory networks on survival in patients with castration-resistant prostate cancer. Br J Cancer. 2017;117:409–20.
12. Koshizuka K, Nohata N, Hanazawa T, Kikkawa N, Arai T, Okato A, et al. Deep sequencing-based microRNA expression signatures in head and neck squamous cell carcinoma: dual strands of pre-miR-150 as antitumor miRNAs. Oncotarget . 2017;8:30288–304.
13. Mizuno K, Mataki H, Arai T, Okato A, Kamikawaji K, Kumamoto T, et al. The microRNA expression signature of small cell lung cancer: tumor suppressors of miR-27a-5p and miR-34b-3p and their targeted oncogenes. J Hum Genet. 2017;62:671–78.
14. Yonemori K, Seki N, Idichi T, Kurahara H, Osako Y, Koshizuka K, et al. The microRNA expression signature of pancreatic ductal adenocarcinoma by RNA sequencing: anti-tumour functions of the microRNA-216 cluster. Oncotarget . 2017;8:70097–115.
15. Toda H, Kurozumi S, Kijima Y, Idichi T, Shinden Y, Yamada Y, et al. Molecular pathogenesis of triple-negative breast cancer based on microRNA expression signatures: antitumor miR-204-5p targets AP1S3. J Hum Genet. 2018;63:1197–210.
16. Yonemori K, Seki N, Kurahara H, Osako Y, Idichi T, Arai T, et al. ZFP36L2 promotes cancer cell aggressiveness and is regulated by antitumor microRNA-375 in pancreatic ductal adenocarcinoma. Cancer Sci. 2017;108:124–35.
17. Idichi T, Seki N, Kurahara H, Yonemori K, Osako Y, Arai T, et al. Regulation of actin-binding protein ANLN by antitumor miR-217 inhibits cancer cell aggressiveness in pancreatic ductal adenocarcinoma. Oncotarget . 2017;8:53180–93.
18. Idichi T, Seki N, Kurahara H, Fukuhisa H, Toda H, Shimonosono M, et al. Molecular pathogenesis of pancreatic ductal adenocarcinoma: Impact of passenger strand of pre-miR-148a on gene regulation. Cancer Sci. 2018;109:2013–26.
19. Idichi T, Seki N, Kurahara H, Fukuhisa H, Toda H, Shimonosono M, et al. Involvement of anti-tumor miR-124-3p and its targets in the pathogenesis of pancreatic ductal adenocarcinoma: direct regulation of ITGA3 and ITGB1 by miR-124-3p. Oncotarget . 2018;9:28849–65.
20. Yamada Y, Arai T, Sugawara S, Okato A, Kato M, Kojima S, et al. Impact of novel oncogenic pathways regulated by antitumor miR-451a in renal cell carcinoma. Cancer Sci. 2018;109:1239–53.
21. Yamada Y, Sugawara S, Arai T, Kojima S, Kato M, Okato A, et al. Molecular pathogenesis of renal cell carcinoma: Impact of the anti-tumor miR-29 family on gene regulation. Int J Urol. 2018;25:953–65.
22. Osako Y, Seki N, Koshizuka K, Okato A, Idichi T, Arai T, et al. Regulation of SPOCK1 by dual strands of pre-miR-150 inhibit cancer cell migration and invasion in esophageal squamous cell carcinoma. J Hum Genet. 2017;62:935–44.
23. Sugawara S, Yamada Y, Arai T, Okato A, Idichi T, Kato M, et al. Dual strands of the miR-223 duplex (miR-223-5p and miR-223-3p) inhibit cancer cell aggressiveness: targeted genes are involved in bladder cancer pathogenesis. J Hum Genet. 2018;63:657–68.
24. Yamada Y, Arai T, Kojima S, Sugawara S, Kato M, Okato A, et al. Regulation of antitumor miR-144-5p targets oncogenes: Direct regulation of syndecan-3 and its clinical significance. Cancer Sci. 2018;109:2919–36.
25. Arai T, Kojima S, Yamada Y, Sugawara S, Kato M, Yamazaki K, et al. Pirin: a potential novel therapeutic target for castration-resistant prostate cancer regulated by miR-455-5p. Mol Oncol. 2019;13:322–37.
26. Cerami E, Gao J, Dogrusoz U, Gross BE, Sumer SO, Aksoy BA, et al. The cBio cancer genomics portal: an open platform for exploring multidimensional cancer genomics data. Cancer Discov. 2012;2:401–4.
27. Gao J, Aksoy BA, Dogrusoz U, Dresdner G, Gross B, Sumer SO, et al. Integrative analysis of complex cancer genomics and clinical profiles using the cBioPortal. Sci Signal. 2013;6:pl1.
28. Anaya J. OncoLnc: linking TCGA survival data to mRNAs, miRNAs, and lncRNAs. PeerJ Comput Sci. 2016;2:e67.
29. Mah SM, Buske C, Humphries RK, Kuchenbauer F. miRNA*: a passenger stranded in RNA-induced silencing complex? Crit Rev Eukaryot Gene Expr. 2010;20:141–8.
30. Yang J, Zeng Y. Identification of miRNA-mRNA crosstalk in pancreatic cancer by integrating transcriptome analysis. Eur Rev Med Pharmacol Sci. 2015;19:825–34.
31. Yang C, Cai J, Wang Q, Tang H, Cao J, Wu L, et al. Epigenetic silencing of miR-130b in ovarian cancer promotes the development of multidrug resistance by targeting colony-stimulating factor 1. Gynecol Oncol. 2012;124:325–34.
32. Egawa H, Jingushi K, Hirono T, Ueda Y, Kitae K, Nakata W, et al. The miR-130 family promotes cell migration and invasion in bladder cancer through FAK and Akt phosphorylation by regulating PTEN. Sci Rep. 2016;6:20574.
33. Ramalho-Carvalho J, Graca I, Gomez A, Oliveira J, Henrique R, Esteller M, et al. Downregulation of miR-130b~301b cluster is

mediated by aberrant promoter methylation and impairs cellular senescence in prostate cancer. J Hematol Oncol. 2017;10:43.
34. Yu T, Cao R, Li S, Fu M, Ren L, Chen W, et al. MiR-130b plays an oncogenic role by repressing PTEN expression in esophageal squamous cell carcinoma cells. BMC Cancer. 2015;15:29.
35. Zhang Q, Zhang B, Sun L, Yan Q, Zhang Y, Zhang Z, et al. MicroRNA-130b targets PTEN to induce resistance to cisplatin in lung cancer cells by activating Wnt/beta-catenin pathway. Cell Biochem Funct. 2018;36:194–202.
36. Dong P, Karaayvaz M, Jia N, Kaneuchi M, Hamada J, Watari H, et al. Mutant p53 gain-of-function induces epithelial-mesenchymal transition through modulation of the miR-130b-ZEB1 axis. Oncogene . 2013;32:3286–95.
37. Dettmer MS, Perren A, Moch H, Komminoth P, Nikiforov YE, Nikiforova MN. MicroRNA profile of poorly differentiated thyroid carcinomas: new diagnostic and prognostic insights. J Mol Endocrinol. 2014;52:181–9.
38. Zhao G, Zhang JG, Shi Y, Qin Q, Liu Y, Wang B, et al. MiR-130b is a prognostic marker and inhibits cell proliferation and invasion in pancreatic cancer through targeting STAT3. PLoS ONE. 2013;8:e73803.
39. Fazioli F, Minichiello L, Matoska V, Castagnino P, Miki T, Wong WT, et al. Eps8, a substrate for the epidermal growth factor receptor kinase, enhances EGF-dependent mitogenic signals. EMBO J. 1993;12:3799–808.
40. Logue JS, Cartagena-Rivera AX, Baird MA, Davidson MW, Chadwick RS, Waterman CM. Erk regulation of actin capping and bundling by Eps8 promotes cortex tension and leader bleb-based migration. eLife . 2015;4:e08314.
41. Chen H, Wu X, Pan ZK, Huang S. Integrity of SOS1/EPS8/ABI1 tri-complex determines ovarian cancer metastasis. Cancer Res. 2010;70:9979–90.
42. Maa MC, Lee JC, Chen YJ, Chen YJ, Lee YC, Wang ST, et al. Eps8 facilitates cellular growth and motility of colon cancer cells by increasing the expression and activity of focal adhesion kinase. J Biol Chem. 2007;282:19399–409.
43. Chen C, Liang Z, Huang W, Li X, Zhou F, Hu X, et al. Eps8 regulates cellular proliferation and migration of breast cancer. Int J Oncol. 2015;46:205–14.
44. He YZ, Liang Z, Wu MR, Wen Q, Deng L, Song CY, et al. Overexpression of EPS8 is associated with poor prognosis in patients with acute lymphoblastic leukemia. Leuk Res. 2015;39:575–81.
45. Li Q, Bao W, Fan Q, Shi WJ, Li ZN, Xu Y, et al. Epidermal growth factor receptor kinase substrate 8 promotes the metastasis of cervical cancer via the epithelial-mesenchymal transition. Mol Med Rep. 2016;14:3220–8.